Anisotropic magnetoresistance in epitaxial La0.67(Ca1−xSrx)0.33MnO3 films

Yiwei Liu, Zhihuan Yang, Huali Yang, Yali Xie, Sadhana Katlakunta, Bin Chen, Qingfeng Zhan, and Run-Wei Li

Citation: Journal of Applied Physics **113**, 17C722 (2013); doi: 10.1063/1.4798798
View online: http://dx.doi.org/10.1063/1.4798798
View Table of Contents: http://scitation.aip.org/content/aip/journal/jap/113/17?ver=pdfcov
Published by the AIP Publishing

Anisotropic magnetoresistance in epitaxial $La_{0.67}(Ca_{1-x}Sr_x)_{0.33}MnO_3$ films

Yiwei Liu, Zhihuan Yang, Huali Yang, Yali Xie, Sadhana Katlakunta, Bin Chen, Qingfeng Zhan,[a] and Run-Wei Li[b]

Key Laboratory of Magnetic Materials and Devices, Ningbo Institute of Material Technology and Engineering (NIMTE), Chinese Academy of Sciences (CAS), Ningbo 315201, People's Republic of China and Zhejiang Province Key Laboratory of Magnetic Materials and Application Technology, Ningbo Institute of Material Technology and Engineering (NIMTE), Chinese Academy of Sciences (CAS), Ningbo 315201, People's Republic of China

(Presented 17 January 2013; received 1 November 2012; accepted 7 January 2013; published online 3 April 2013)

We investigated the anisotropic magnetoresistance (AMR) effects for $La_{0.67}(Ca_{1-x}Sr_x)_{0.33}MnO_3$ films epitaxially grown on (001) oriented $SrTiO_3$ substrates. The increase of Sr doping gives rise to the enhancement of the metal-insulator transition temperature, but suppresses the AMR amplitude. The dependence of AMR on the magnetic field orientation for the Sr doping samples shows the coexistence of two-fold and four-fold symmetries, which is changed with varying the temperature. Moreover, the sign of AMR is changed from negative to positive with increasing the temperature. The abnormal AMR behaviors can be understood by different *s-d* scattering occurring at different temperatures. © *2013 American Institute of Physics*. [http://dx.doi.org/10.1063/1.4798798]

Anisotropic magnetoresistance (AMR) is defined as the dependence of resistance on angle between the magnetization and the direction of current flow or a crystal axis.[1] In conventional ferromagnetic (FM) metals or alloys, such as permalloy an AMR ratio of 2%–3% can be achieved at room temperature,[2] which has been widely used in magnetic sensors and magnetic read-heads.[3] However, after the discovery of giant magnetoresistance (GMR), whose value can reach 8% at room temperature, the AMR magnetic read-heads are gradually replaced by the GMR magnetic read-heads.[4] Since AMR devices possess a simple structure and can be easily fabricated, many efforts have been made to search for new materials with the high AMR ratio. Recently, AMR in perovskite manganites (single crystal, epitaxial films, and polycrystalline samples) have attracted a lot of interests due to their large AMR ratio (10% to 90%) compared with the conventional ferromagnetic metals or alloys.[5–10] The maximum AMR ratio in perovskite manganites usually appears at the metal-insulator transition (MIT) temperature, which is normally below the room-temperature.[5–10] It is well known that the Sr doping in $La_{0.67}Ca_{0.33}MnO_3$ can improve the MIT temperature to room-temperature.[11] Moreover, the Sr doping in perovskite manganites can also tune the lattice constant and the couplings between spin, charge, orbital, and lattice,[12] which can affect MIT, colossal magnetoresistance, charge-orbital ordering, phase separation, and AMR.[13] In this paper, we systematically studied the AMR behaviors in epitaxial $La_{0.67}(Ca_{1-x}Sr_x)_{0.33}MnO_3$ (LCSMO) films. AMR is changed from negative to positive with increasing the temperature, which can be understood by different *s-d* scattering at low and high temperatures.

$La_{0.67}(Ca_{1-x}Sr_x)_{0.33}MnO_3$ ($x = 0.0$, 0.33, and 0.67) films were epitaxially grown on (001)-$SrTiO_3$ substrates by pulsed-laser deposition using $La_{0.67}Ca_{0.33}MnO_3$ and $La_{0.67}Sr_{0.33}MnO_3$ targets. Periods of $La_{0.67}Ca_{0.33}MnO_3$/$La_{0.67}Sr_{0.33}MnO_3$ bilayers with the thickness ratio of 4 nm/2 nm and 2 nm/4 nm, respectively, were deposited for the fabrication of LCSMO films with $x = 0.33$ and 0.67. The total thickness is set at 120 nm. All the films were annealed at 850 °C under an oxygen atmosphere of 1 atm for 1 h. The morphology of the films was characterized by scanning electron microscopy (SEM). The transport properties were measured by Physical Property Measurement System (PPMS, Quantum Design) with a conventional four-point probe technique. During the measurements, the magnetic field was rotated within the plane perpendicular to the current flow direction and the resistance was measured as a function of the angle (θ) between the magnetic field and the normal of LCSMO films. The AMR(θ) is defined as $[R(\theta)/R(0)-1] \times 100\%$, where $R(\theta)$ and $R(0)$ represent the resistance at θ and $\theta = 0°$, respectively. The AMR amplitude is the maximum of AMR(θ).

The resistance, R, and the differential coefficient, $dR(T)/dT$, as a function of temperature for LCSMO films are shown in Figs. 1(a) and 1(b), respectively. The MIT temperature, T_{MI}, is defined at the temperature where $dR(T)/dT$ shows a maximum. It is seen that T_{MI} of LCSMO film with $x = 0$, i.e., $La_{0.67}Ca_{0.33}MnO_3$, is 261 K. The paramagnetic (PM) insulating and FM metallic phases coexist when the temperature is near T_{MI}.[14] T_{MI} is usually increased with increasing the Sr doping in LCSMO. For our LCSMO films, dual T_{MI} are observed to appear at 283 and 298 K for $x = 0.33$, and 313 and 328 K for $x = 0.67$. The dark and bright regions in the SEM image of the sample with $x = 0.67$ indicate the different conducting properties of LCSMO film, as shown in the inset of Fig. 1(a). The energy dispersive X-ray spectroscopy shows that the white region contains more Sr than the dark region. It is well known that both Ca and Sr occupy A positions of ABO_3 perovskite lattice.[15] In our samples, Sr in A

[a]Electronic mail: zhanqf@nimte.ac.cn
[b]Electronic mail: runweili@nimte.ac.cn

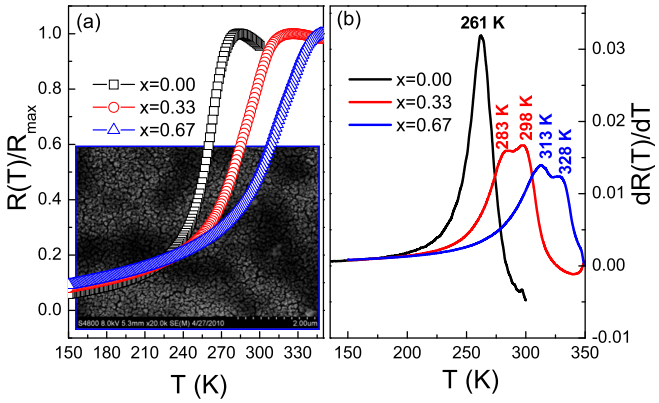

FIG. 1. (a) The resistance, R, and (b) the differential coefficient, $dR(T)/dT$, as a function of temperature for LCSMO films with $x = 0$, 0.33, and 0.67. The inset shows the SEM morphology for LCSMO film with $x = 0.67$.

positions is obviously not distributed uniformly, which is likely caused by the insufficient diffusion of Sr during the annealing process. The dual T_{MI} may originate from the two different regions with different Sr contents.

The AMR for LCSMO films at different temperatures are shown in Fig. 2. For LCSMO with $x = 0$, i.e., $La_{0.67}Ca_{0.33}MnO_3$ (LCMO), the AMR amplitude reaches a maximal value of 6.6% at 263 K near T_{MI} under a magnetic field of 5 kOe, and when the temperature is far away from T_{MI}, the value of AMR decreases rapidly. The similar behavior is also observed in other perovskite manganite films.[5–7] For LCSMO with $x = 0.33$ and 0.67 under 5 kOe, when the temperature is near the low T_{MI} (283 K for $x = 0.33$ and 313 K for $x = 0.67$), the AMR ratio reaches the maximum values of 1% and 1.3% at 280 and 300 K, respectively, which are much smaller than the value of LCMO film. When the temperature is increased close to the high T_{MI} (298 K for $x = 0.33$ and 328 K for $x = 0.67$), the sign of AMR is changed from negative to positive. Figure 2(d) shows the temperature and angular dependences of AMR for LCSMO with $x = 0.67$ at 5 kOe. It is clearly seen that the negative and positive maximal values appear at the temperatures close to the low T_{MI} at 313 K and the high T_{MI} at 328 K, respectively.

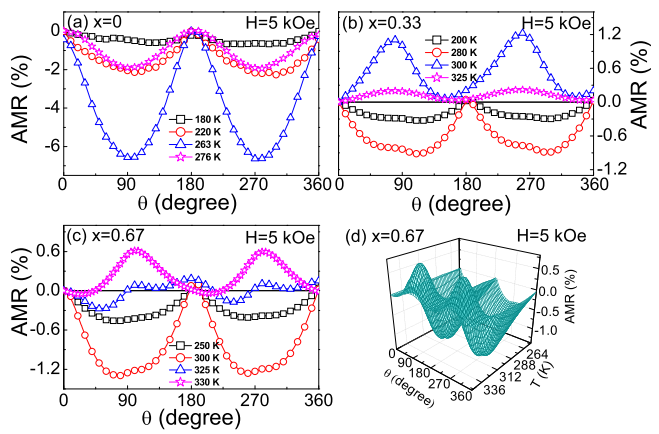

FIG. 2. Angular dependence of AMR for LCSMO films with (a) $x = 0$, (b) $x = 0.33$, and (c) $x = 0.67$ at various temperatures under a magnetic field of 5 kOe. (d) Temperature and angular dependence of AMR for LCSMO films with $x = 0.67$ under 5 kOe.

Figures 3(a)–3(d) show AMR at 250, 310, 325, and 330 K under various magnetic fields for LCSMO with $x = 0.67$. When the temperature is lower than the low T_{MI}, the AMR amplitude is negative and a maximum value of 1.4% is found at 310 K under 3 kOe. For the temperature near the high T_{MI}, for example, 325 and 330 K, AMR shows a positive value at a rather low magnetic field. The AMR curves can be well expressed by the equation $K_0 + K_1\cos(2\theta + \varphi_0) + K_2\cos(4\theta + \varphi_1)$, as seen in Fig. 3, which clearly shows that the symmetry of AMR is the combination of two-fold and four-fold ones,[16] where K_1 and K_2 represent the amplitudes of two-fold and four-fold symmetric AMR, respectively, and K_0, φ_0, φ_1 are the coefficients. With increasing the magnetic field, the four-fold symmetric part is decreased. Under the high magnetic field, such as 50 kOe, only the two-fold symmetric contribution is observed.

The temperature dependence of the AMR fitting results of K_1 and K_2 for LCSMO with x = 0.67 are shown in Fig. 4. At low temperature, both K_1 and K_2 are positive and K_1 is larger than K_2. With increasing the temperature, both K_1 and K_2 are increased and reach their maximal values near the low T_{MI} at 313 K. With increasing the temperature from 313 to 328 K, both K_1 and K_2 are decreased and equal at 325 K. With further increasing the temperature, K_2 becomes larger than K_1, and the sign of K_1 is changed from positive to negative and the absolute value of K_1 is larger than K_2. At the high temperature, both K_1 and K_2 are decreased to zero. The variation of K_1 and K_2 with the temperature indicates the competition between the uniaxial anisotropy and the magneto-crystalline anisotropy of LCSMO, which gives rise to the complicated AMR behaviors at various temperatures.

The origin of AMR can be understood by *s-d* scattering from conductive *s*-states to localized *d*-states hybridized by spin-orbit interaction.[17–19] In perovskite manganites, the electric current is carried by *d*-electrons hopping between neighboring manganese sites according to the double-exchange model.[20] Therefore, the conductive *s*-states in perovskite manganites are mostly contributed by the conductive *d*-electrons. Theoretically, the sign of AMR is determined by the factor of $f = -(m_\downarrow^4/m_\uparrow^4 - D_\downarrow^{(d)}/D_\uparrow^{(d)})$,[21] where $D_\uparrow^{(d)}$ and $D_\downarrow^{(d)}$ are the density of states (DOS) at the Fermi energy E_F for the spin-up and spin-down localized *d*-state electrons,

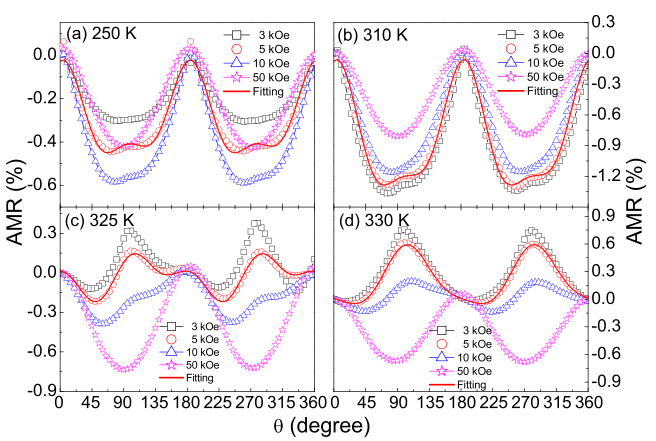

FIG. 3. Angular dependence of AMR for LCSMO films with $x = 0.67$ at (a) 250 K, (b) 310 K, (c) 325 K, and (d) 330 K under various magnetic fields.

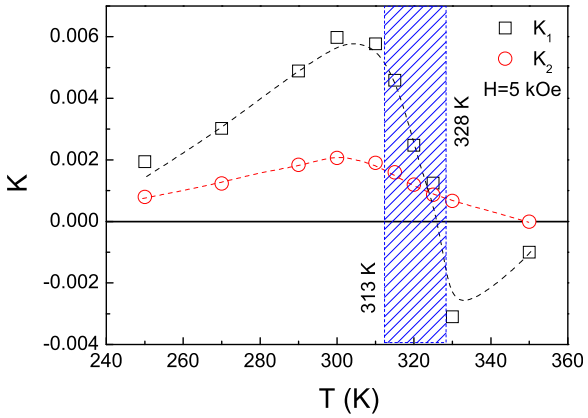

FIG. 4. Temperature dependence of the AMR fitting results of K_1 and K_2 for LCSMO with x = 0.67 under a magnetic field of 5 kOe.

respectively, and $m_\uparrow$ and $m_\downarrow$ are the effective mass of the spin-up and spin-down conductive *s*-state electrons, respectively. In LCSMO films, the *s-d* scattering is strongly affected by the structure and the lattice distortion. It is well known that LCSMO possesses a rhombohedral to pseudo-cubic structural phase transition with increasing the Sr doping, and the tolerance factor of LCSMO is accordingly increased as well.[22] For the rhombohedral LCSMO with low Sr doping, the *d*-orbital states are different when magnetic field applied at $\theta = 0°$ and 90°, leading to the anisotropic *s-d* scattering and a two-fold symmetric AMR. The cubic magneto-crystalline anisotropy appears in the pseudo-cubic LCSMO with high Sr doping and therefore induces a four-fold symmetric AMR. Due to the large tolerance factor of LCSMO at high Sr doping, the distortion of *d*-orbit is weak, so AMR caused by the anisotropic *s-d* scattering is accordingly reduced.[11] Since the magnetic field is rotated out of plane during measurement, the shape anisotropy due to the demagnetization effect results in an uniaxial anisotropy and two-fold symmetric AMR. Therefore, for LCSMO with $x = 0.33$ and $x = 0.67$, the superimposition of two-fold and four-fold symmetric AMR can be understood by combining the demagnetization effect and magneto-crystalline anisotropy. At low temperature, $D_\uparrow^{(d)} \gg D_\downarrow^{(d)}$ and $m_\downarrow/m_\uparrow$ is a finite value about 0.1 (Ref. 21) and the main scattering is from conductive spin-up *s*-state electrons to spin-up *d*-state electrons, i.e., $s_\uparrow \rightarrow d_\uparrow$, therefore, both *f* and AMR are negative. With increasing the temperature, the enhanced lattice distortion may increase the difference in *d*-orbital states when magnetic field is applied along different lattice direction; therefore, both the anisotropic *s-d* scattering and AMR are increased.[8] When the temperature is around the high T_{MI} of 328 K, LCSMO is in a phase-separated state, that is, FM clusters are separated with each other,[23] and the demagnetizing field of the FM clusters becomes even weak. The four-fold symmetric AMR induced by the cubic crystalline anisotropy becomes visible. With further increasing the temperature, the DOS of minority spin is increased, which enhances the scattering from conductive spin-up *s*-state electrons to spin-down *d*-state electrons ($s_\uparrow \rightarrow d_\downarrow$ scattering[24]) and therefore results in a positive *f* and a positive AMR at high temperature. It is noticed that, regardless of the temperature, the AMR under a high magnetic field of 50 kOe shows a two-fold symmetry, as shown in Figs. 3(a)–3(d). At low temperature, for the magnetic field larger than the magneto-crystalline anisotropy field, the *d*-orbital states are different for magnetic field applied along $\theta = 0°$ and 90° due to the demagnetizing effect; thus, a two-fold symmetric AMR is induced by anisotropic *s-d* scattering. For temperature near T_{MI}, due to the metamagnetic transition, the PM clusters are changed to the FM clusters under a high magnetic field of 50 kOe;[25,26] therefore, the demagnetizing field becomes dominant again and the anisotropic *s-d* scattering induces a two-fold symmetric AMR by applying a high magnetic field.

The authors acknowledge the financial support from the National Natural Foundation of China (11274321, 11174302), the State Key Project of Fundamental Research of China (2012CB933004, 2009CB930803), the Chinese Academy of Sciences (CAS), and the Ningbo Science and Technology Innovation Team (2011B82004, 2009B21005), the Projects of Nonprofit Technology and Research in Zhejiang Province (2010C31041), and the Zhejiang and Ningbo Natural Science Foundations.

[1]T. McGuire and R. Potter, IEEE Trans. Magn. **11**, 1018 (1975).
[2]Th. G. S. M. Rijks *et al.*, Phys. Rev. B **56**, 362 (1997).
[3]T. Jungwirth *et al.*, Rev. Mod. Phys. **78**, 809 (2006).
[4]A. Fert, Rev. Mod. Phys. **80**, 1517 (2008).
[5]R. W. Li *et al.*, Proc. Natl. Acad. Sci. U.S.A. **106**, 14224 (2009).
[6]W. Ning *et al.*, Appl. Phys. Lett. **98**, 212503 (2011).
[7]J. O. Donnell *et al.*, Appl. Phys. Lett. **76**, 218 (2000).
[8]M. Bibes *et al.*, J. Phys. Condens. Matter. **17**, 2733 (2005).
[9]M. Egilmez *et al.*, Appl. Phys. Lett. **90**, 232506 (2007).
[10]M. Egilmez *et al.*, J. Appl. Phys. **105**, 07D706 (2009).
[11]Y. W. Liu *et al.*, J. Phys. D: Appl. Phys. **45**, 245001 (2012)
[12]E. Dagotto, Science **309**, 257 (2005).
[13]J. Mira *et al.*, Phys. Rev. B **60**, 2998 (1999).
[14]A. K. Pradhan *et al.*, Appl. Phys. Lett. **79**, 506 (2001).
[15]C. N. R. Rao *et al.*, Chem. Mater. **8**, 2421 (1996).
[16]C. Bihler *et al.*, Phys. Rev. B **75**, 214419 (2007).
[17]J. Smit, Physica **17**, 612 (1951).
[18]I. A. Campbell *et al.*, J. Phys. C: Solid State Phys. **3**, S95 (1970).
[19]A. P. Malozemoff, Phys. Rev. B **34**, 1853 (1986).
[20]J. D. Fuhr *et al.*, J. Phys.: Condens. Matter. **22**, 146001 (2010).
[21]S. Kokado *et al.*, J. Phys. Soc. Jpn. **81**, 024705 (2012).
[22]K. X. Jin *et al.*, Mater. Sci. Eng. B **119**, 206 (2005).
[23]R. W. Li *et al.*, Appl. Phys. Lett. **80**, 3367 (2002).
[24]F. J. Yang *et al.*, Phys. Rev. B **86**, 020409(R) (2012).
[25]M. Bibes *et al.*, J. Magn. Magn. Mater. **211**, 206 (2000).
[26]P. Li *et al.*, J. Appl. Phys. **108**, 093921 (2010).